白金イリジウム線の交流電解研磨における周波数依存性

青 山 宜 樹[*1]，高 見 知 秀[*2]

Frequency dependence of alternate current electrochemical etching of platinum/iridium wire

Yoshiki AOYAMA[*1] and Tomohide TAKAMI[*2]

Abstract

白金イリジウム線を交流電解研磨したときの交流周波数依存性について調べた．周波数が100ヘルツから1000ヘルツに増加するにつれて反応速度は増加したが，交流による電極の変化に依存する反応持続時間は減少した．このため，作製された探針の細くなっている部分の長さは長くなり，研磨された部分の根元での抉れは大きくなった．更に10000ヘルツになると，アノードとカソードが交互に入れ替わる周期が早くなるため研磨が不十分になり，研磨している探針表面に塩化白金が不動態として残った．上記の3つの周波数での比較では，1000ヘルツのときが最も良好な研磨となり，走査トンネル顕微鏡の探針として用いたときに最も良質な像を得ることができた．

Keywords: Platinum Iridium, Scanning Tunneling Microscopy, Electrochemical Etching

1. Introduction

Scanning tunneling microscopy (STM)[1-8] has been contributed to the development of surface science and nanotechnology. In STM, sharp metal tip is the gate of nano-signal and the most important part. Just a cut tip with diagonals is available to use for STM observation with atomic resolution on an atomically flat surface. On the surface with roughness or steps, however, the tunneling point of the STM tip changes during the scanning, which result in the ghost image attributed to the multi-tip effect.[9] Moreover, the variation of STM such as photon STM,[10-13] STM induced luminescence,[14] tip-enhanced Raman scattering spectroscopy,[15] and electrochemical STM[16-18] requires sharp and symmetric STM tip. Therefore, the fabrication of atomically sharp and symmetric STM tip is needed for the application of the STM to the various kinds of the method of nanoscale surface observation and manipulation.[19]

Platinum-iridium (PtIr) alloy wire is widely used for the STM tip. Although KCN solution can be used for the etching of PtIr,[20,21] alternate current (AC) etching with alkali chloride solution is widely used to get rid of using toxic solution.[22-24] Czerepak showed the detail method of AC tip etching of PtIr wire.[25] Zhang and Lian discussed the behavior during the AC tip etching.[26] Vitus *et al.* showed the light emission spectra of sparking during the etching and confirmed all the elements in the etching process.[27] Libioulle *et al.* conducted additional micro polishing with H_2SO_4 *aq.* solution after the AC tip etching.[28] Kupper added acetone in the $CaCl_2$ solution to make the hydrogen bubble smaller during the AC tip etching.[29]

However, the chemical reaction mechanism of AC tip etching is still ambiguous because the AC frequency dependence of the etching reaction has not been investigated. Moreover, the mechanism of the chemical reaction to produce platinum chlorides, the by-products from the AC tip etching of PtIr wire, is still not elucidated.

In this paper, the AC frequency dependence of the chemical etching of PtIr wire has been reported. The

[*1] 工学院大学工学部応用化学科2017年卒業　Department of Applied Chemistry, Kogakuin University
[*2] 工学院大学教育推進機構ナノ化学研究室教授　Nanotechnology Chemistry Laboratory, Division of Liberal Arts, Kogakuin University

PtIr tips were produced with the AC electrochemical etching at 100, 1000, and 10000 Hz. The produced tips were observed with scanning electron microscopy (SEM), and were evaluated from the observed STM images using the tips. Moreover, 4-pyridinecarboxylic acid – pyrazolone was used for the determination of chlorine gas from the trapped gas during the etching, and ion chromatography was applied for the determination of chloric acids in the solution after the etching.

2. Experimental methods

Platinum iridium (80:20) wire with 0.20 mm diameter and nickel ribbon with 0.20 mm thick and 7.0 mm wide were purchased from Nilaco Co. Ltd. The water solvent used in this study was produced with Organo BB-5B/G-35PA, and the typical specific resistance was 5 MΩ·cm. Potassium chloride (Yanagishima Pharmaceutical Co. Ltd., special grade, >99.5%) was dissolved in the prepared water to produce 1.5 M KCl solution used for the electrochemical etching.

Figure 1(a) shows the apparatus for the AC electrochemical etching. The body was formed with a plastic kit (Tamiya universal joint), and the PtIr wire was held with an alminum sharp pencil body (Steadtler, type 0.3 mm) as a probe holder. Nickel ribbon was fabricated to ring-shape and set in a glass dish in order to apply symmetric electric potential to PtIr wire.

(a)

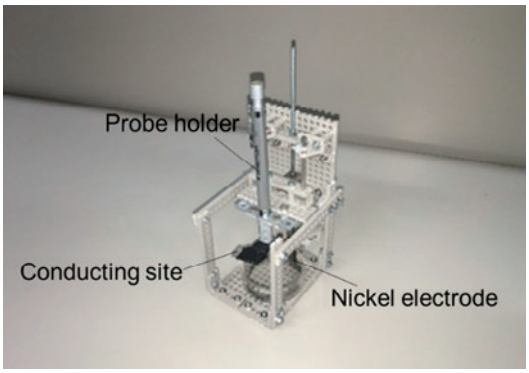

(b)

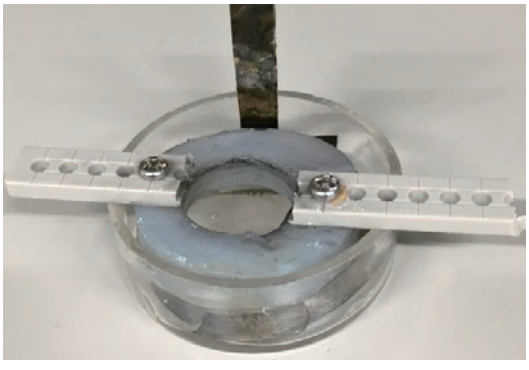

Fig.1 (Color online) The apparatus for the AC electrochemical etching (a) and the tool to remove bubbles from the PtIr wire during the etching process (b)

Figure 1(b) shows the tool to remove bubbles from the PtIr wire during the etching process. Donuts-shape silicone rubber surrounding the PtIr wire was set on the solution surface. In this way, the bubbles formed around the PtIr wire were removed from the wire with the point symmetry.

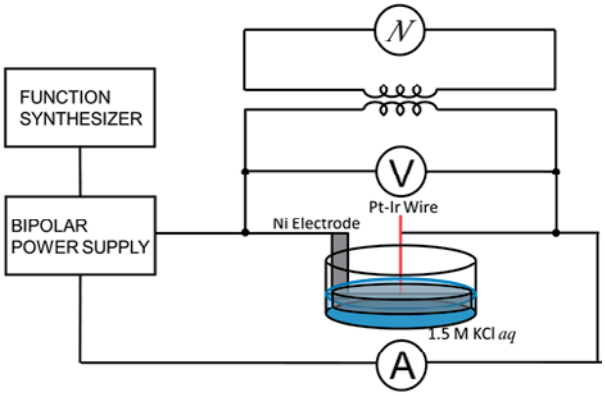

Fig.2 (Color online) The schematics showing the circuit for the AC etching.

Figure 2 shows the circuit for the AC etching. The AC wave was produced with a function synthesizer (NF Electronic Instruments 1915) and it was amplified with a bipolar power supply (NF Electronic Instruments BP4610). The voltage and current during the etching were monitored with digital multimeters (Advantest R6451A and SANWA PC720M), and the AC wave was observed with a digital storage oscilloscope (A&D AD5142D) via an isolation transformer to get rid of the short of the circuit to ground.

After the PtIr wire was set to the holder and the circuit was prepared, 20 mL of 1.5 M KCl solution was poured into the dish with the circle nickel ribbon counter electrode, and the PrIr wire was set in such a way that the wire dipped 5 mm into the solution. Next, 7 V and 100 Hz AC pulse for 1 s was applied to the PtIr wire to wash the surface of the wire. Confirmed the bubbles formed around the PtIr wire, the wire was withdrawn from the solution once. Then the wire was dipped in the solution again for 0.5 mm. After setting the AC voltage to 20 V, the AC voltage was applied to the PtIr wire to start the etching. Figure 3 shows

a typical example, in case of 100 Hz, of the etching current sequence during the etching. The etching started at 0.16 A and the current fluctuated between 20 and 190 s. The current fluctuation was due to the bubbles around the PtIr wire during the etching, and the bubbles caused the decrease of contacting area of the wire to the solution. The large spike at 140 s was due to the large bubble formed around the wire. The frequency of the formation of large bubble could be reduced by using donuts-shape silicone rubber surrounding the PtIr wire as shown in Fig. 1(b). After 190 s, the volume of the formed bubbles and the corresponding current fluctuation was reduced. The falling at 230 s is the point to stop etching because the junction between the wire and the solution got small. It is noted that the amplitude of the sound got small and the frequency of the sound got higher at the point. After the etching, 3 V and 100 Hz AC pulse for 1 s, as shown in Fig. 4, was applied to the etched PtIr tip to wash the tip surface and remove the platinum chlorides formed on the tip surface. Last, the tip was rinsed with distilled water for 3 times. The etching AC frequencies were 100, 1000, and 10000 Hz in this study. The washing AC frequency before and after the etching was unified to 100 Hz at any tip producing processes.

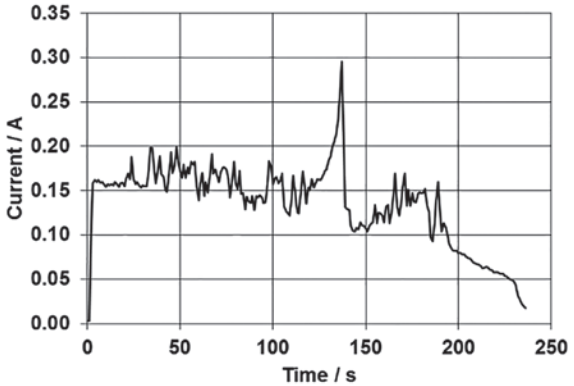

Fig.3 Typical example of the etching current sequence during the etching. Frequency: 100 Hz.

The prepared PtIr tips were observed with SEM (JEOL JSM6380A) and used for STM observation (JEOL JSPM5200). No additional metal deposition was conducted to the PtIr tips for the SEM observation. No smoothing process was conducted to the obtained STM images.

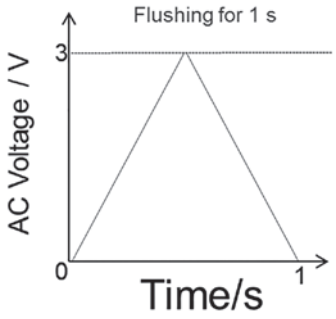

Fig.4 Time sequence of the applied pulse for washing the etched tip.

3. Results and discussion

First, AC etching at 1 Hz was tried in vain. Just DC etching of the following reactions occurred alternately,

Platinum anode: $2Cl^- \rightarrow Cl_2\uparrow + 2e^-$ ····· (1)

Nickel cathode: $2H_2O + 2e^- \rightarrow 2OH^- + H_2\uparrow$ ····· (2)

Platinum cathode: $2H_2O + 2e^- \rightarrow 2OH^- + H_2\uparrow$ ··· (3)

Nickel anode: $Ni \rightarrow Ni^{2+} + 2e^-$ ····· (4)

The following reaction occurs from the reactions (3) and (4),

$Ni^{2+} + 2OH^- \rightarrow Ni(OH)_2\downarrow$ ····· (5)

and the most of the formed Cl_2 gas were dissolved in the solution to produce HClO,

$Cl_2 + H_2O \rightarrow HCl + HClO$ ····· (6)

No etching occurred at 1 Hz; overnight experiment caused the dried up of the solution to produce the powder mixture of KCl, KOH, and $Ni(OH)_2$. The formation of $Ni(OH)_2$ can be confirmed with the light green color powder and the light green color powder can be dissolved in ammonium solution to show blue color of the solution, *i.e.*, the complex $[Ni(NH_3)_6]^{2+}$ was formed.

Table 1 shows the etching time and initial current at the etching AC frequencies of 100, 1000, and 10000 Hz. Though the etching rate increased from 100 Hz to 1000 Hz and the etching time got short, the etching rate decreased from 1000 Hz to 10000 Hz and the etching time got long.

Table 1 The etching time and initial current at each etching AC frequency.

Frequency / Hz	100	1000	10000
Etching time / s	240 ± 30	90 ± 20	270 ± 30
Initial current / A	0.150 ± 0.050	0.200 ± 0.050	0.300 ± 0.100

The AC etching was proceeded with the alternate reactions of oxidation reaction at anode, and hydrogen gas was formed reaction at cathode, resulting in the surface corrosion and removal of surface products by hydrogen gas bubble. The AC frequency is the periodicity of the alternation of the reactions. It is noted that the PtIr wire also vibrated with the frequency of the applied AC voltage and the spreading rate of black platinum chloride powder in the solution was higher at 1000 Hz than at 100 Hz.

The etching current I could be written in the following equation,

$$I = \mathrm{V} / \sqrt{R^2 + \left(\frac{1}{2\pi fc}\right)^2} \quad \cdots\cdots (7)$$

where V is the applied AC voltage, R is the resistance of the solution, f is the AC frequency, and C is the capacitance. It is derived from the equation (7) that the initial current increases with the increase of the frequency, which is in agreement with the values in Table 1.

From the above results, it is predicted that the difference of the etching time at 100 and 1000 Hz is attributed to (i) the supply of reactive flesh solution to the etching wire due to the stirring of the solution from the high frequency vibration of the wire and (ii) the increase of the etching current with the increase of the frequency according to the equation (7).

The SEM images of the produced PtIr tips at each frequency are shown in Fig. 5. The surface roughness was the largest at 100 Hz etching. It is noted that the roughness also related to the applying AC voltage. Zhang and Lian reported that the lower voltage caused the increase of etching time,[26] and Sørensen *et al.* reported that the higher voltage caused the surface roughness and thinness of the etched tip.[30] Actually, compared the produced tip at 1000 Hz with that at 100 Hz, the shank was long and the embankment, concave shape at the root of the etched part, was large, which were confirmed by optical microscope, due to the increase of the etching rate. On the other hand, the duration time of the corrosive reaction was longer at 100 Hz than at 1000 Hz, which results in the tip with no flake at the top and the short shank. In case of 10000 Hz, the tip surface was covered with platinum chlorides caused the charge up in the SEM images.

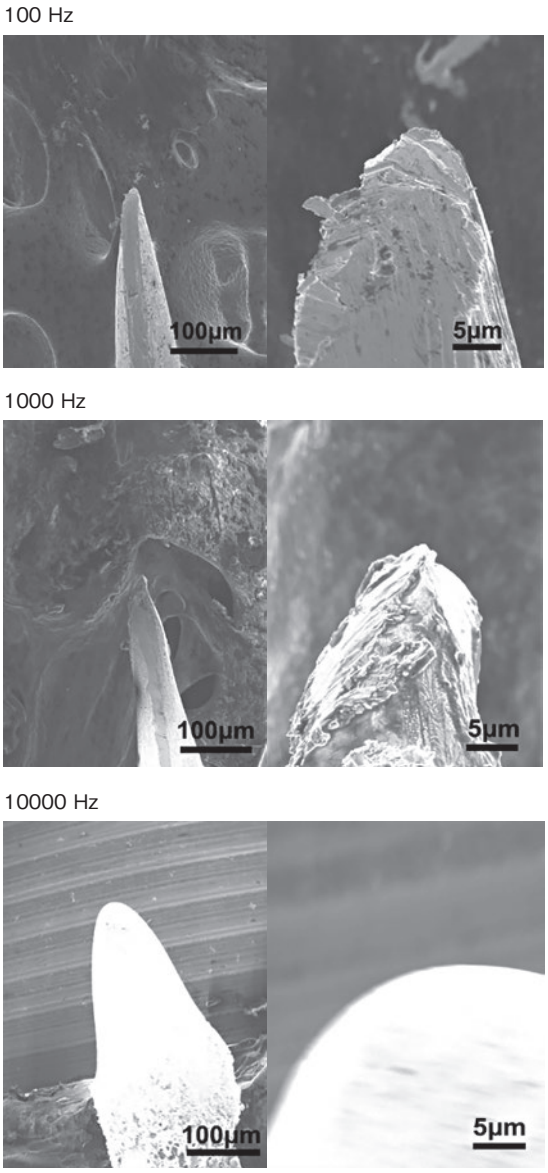

Fig.5 Scanning electron microscope images of prepared PtIr tips at the etching AC frequencies of 100, 1000, and 10000 Hz, respectively. Magnifications: 250x at left column and 3000x at right column.

The tip top was round and the shank was shorter. The amount of produced black powder of platinum chlorides was little, as shown in Fig. 6, which indicates the change in reaction mechanism.

It is predicted from the residues of the etching, as shown in Fig. 6, that the etching reaction was the same at 100 Hz and 1000 Hz, whereas different at 10000 Hz from lower frequencies. Therefore, the residues were investigated with 4-pyridinecarboxylic acid – pyrazolone method using Hitachi U-5100 for the determination of chlorine gas from the trapped gas during the etching, and ion chromatography

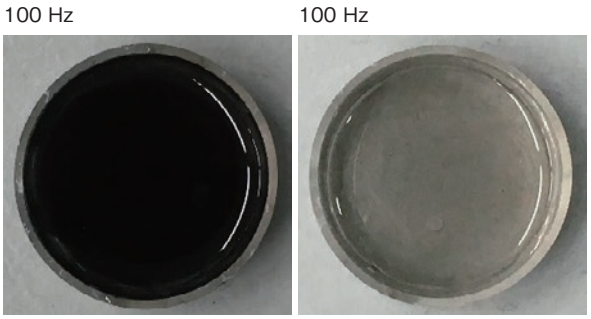

Fig.6 (Color online) Photos of the solutions after AC etching; 100 Hz (left) and 10000 Hz (right). Same solution as 100 Hz was obtained at 1000 Hz.

using Shimadzu LC-20ADsp for the determination of chloric acids in the solution after the etching. These measurements were asked to A-kit, Inc. Unfortunately, the chlorine gas was under the detection limit of 50 vol ppm because most of the produced chlorine gas were dissolved in the solution and changed into HClO. It was also confirmed from the firing of the residue gas that the residue gas was mostly hydrogen. On the other hand, the results from ion chromatography indicated that the concentration of the produced hypochlorite ion in the residue solution was 45 mg/L at 100 Hz and 0.1 mg/L at 10000 Hz, which also indicates that different reaction occurred at 10000 Hz.

The prepared tips were used for the observation of graphite sample with STM. According to the purpose of the evaluation of the STM tips, atomic resolution imaging is not necessary because it can be available using just a cut PtIr tip. Therefore, the imaging at large scale, 500 nm square, was conducted to observe steps in the image. Figure 7 shows the obtained STM images with the tips prepared at 100, 1000, and 10000 Hz. Using the tip prepared at 100 Hz, though the morphology of the graphite step surface can be recognized, the scanning tip frequently touch to the sample, caused the shanking in the image and the shifting of the step lines. Using the tip prepared at 1000 Hz, observed steps were clear and the step edge was sharp compared with the image at 100 Hz. Using the tip prepared at 10000 Hz, the scanning tip contact with the sample many times and the image cannot be used for the sample evaluation. Among the images shown in Fig. 7, the tip prepared at 1000 Hz showed the best image.

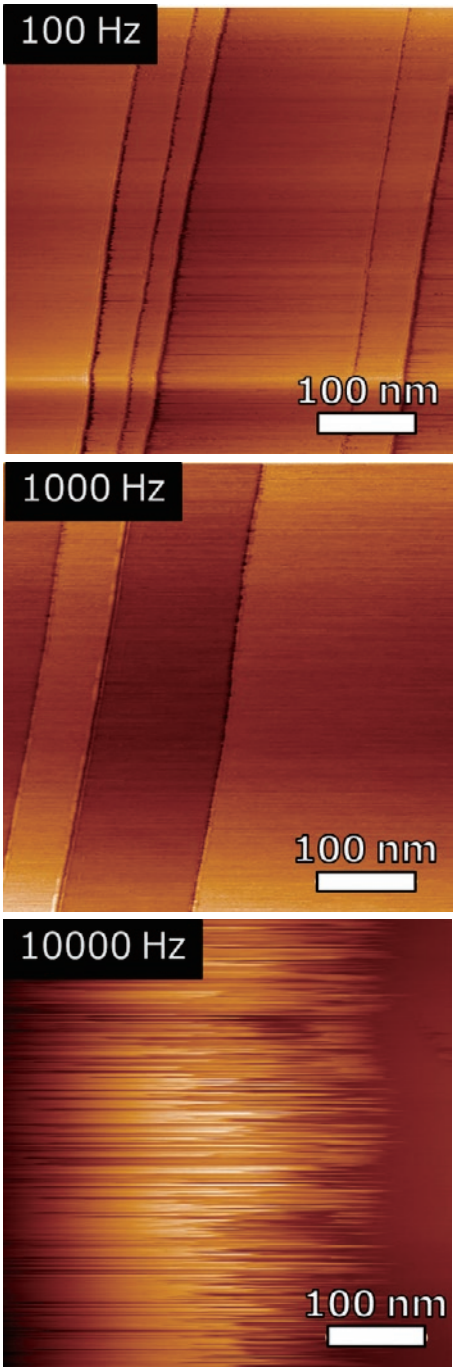

Fig.7 (Color online) Scanning tunneling microscope images of graphite with steps. The AC frequencies used for the prepared PtIr tips: 100 Hz (upper), 1000 Hz (middle), and 10000 Hz (lower). Sample bias voltage: 0.95 V. Tunneling current: 0.02 nA.

Finally, the etching mechanism at each frequency was discussed, as shown in Fig, 8. Sørensen *et al.* proposed the AC etching mechanism. Chloride ions attach to the PtIr wire and the hydrogen gas bubble and heat driven flow climbing up the PtIr wire caused

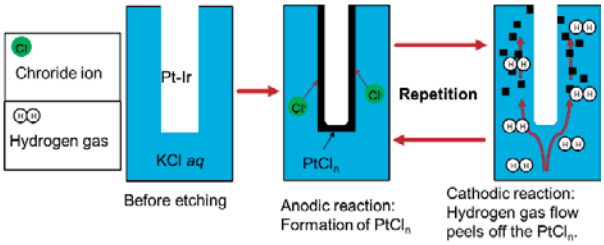

Fig.8 (Color online) Schematics showing the mechanism of AC etching of platinum iridium wire.

the formation of $Pt(IV)Cl_6^{2-}$ at the wire surface.[30] Actually, at the PtIr wire electrode, the production of platinum chlorides and chlorine gas occurred when the electrode is anode, and the production of hydrogen gas occurred when the electrode is cathode. The ion chromatography measurement at 10000 Hz indicates that the above alternate reactions did not occur efficiently, which caused the residual platinum chlorides on the tip surface. As discussed above, the AC etching was proceeded with the alternate switching of the anodic and cathodic reactions of oxidation and hydrogen bubble formation, respectively. At 10000 Hz, the duration time of the hydrogen bubble formation was not enough, resulting in the residue of platinum chlorides on the wire surface and the residue hindered the anodic reaction, which is in agreement with the SEM observation.

4. Conclusion and Remarks

We have observed the frequency dependence of the AC etching for platinum iridium wire for the use of the STM tip. The reaction rate increased from 100 Hz to 1000 Hz, and the shank length of the obtained tip was long and the embankment was deep. At 10000 Hz, the rapid switching of anodic and cathodic reactions resulted in the insufficient etching and the residue of platinum chlorides on the tip surface. It is concluded from the STM observation that the PtIr tip prepared at 1000 Hz shows the best image compared with those at 100 and 10000 Hz.

The gas collection process was not enough to detect chlorine gas in this study. Further improvement aimed for the gas collection may elucidate the reaction process in detail. We are also preparing the easier and low-cost apparatus using a conventional guitar amplifier for the AC etching.

Acknowledgment

This work was supported by JSPS KAKENHI Grant Number 15K04678.

References

1) G. Binnig and H. Rohrer, Helv. Phys. Acta **55**, 726 (1982).
2) G. Binnig, H. Rohrer, Ch. Gerber, and E. Weibel, Phys. Rev. Lett. **49**, 57 (1982)
3) G. Binnig, H. Rohrer, Ch. Gerber, and E. Weibel, Phys. Rev. Lett. **50**, 120 (1983).
4) G. Binnig and H. Rohrer, Rev. Mod. Phys. **59**, 615 (1987).
5) M. Aono, A. Kobayashi, F. Grey, H. Uchida, and D.-H. Huang, Jpn. J. Appl. Phys. **32**, 1470 (1993).
6) Y. Kuk, e-J. Surf. Sci. Nanotech. **12**, 133 (2014).
7) K. Takayanagi, e-J. Surf. Sci. Nanotech. **12**, 149 (2014).
8) G. Le Lay, e-J. Surf. Sci. Nanotech. **12**, 189 (2014).
9) R. Wiesendanger and H. -J. Güntherodt, *Scanning Tunneling Microscopy II* (Springer, Berlin, 1995) p.60.
10) J. M. Vigoureux, D. Courjon, and C. Girard, Optics Lett. **14**, 1039 (1989).
11) R. C. Reddick, R. J. Warmack, and T. L. Ferrell, Phys. Rev. B. **39**, 767 (1989).
12) W. Adams, M. Sadatgol, and D. Ö. Güney, AIP Advances **6**, 100701 (2016).
13) C. Ropers1, C. C. Neacsu, M. B. Raschke, M. Albrecht, C. Lienau, and T. Elsaesser. Jpn. J. Appl. Phys. **47**, 6051 (2008).
14) C. Zhang, L. Chen, R. Zhang, and Z. Dong, Jpn. J. Appl. Phys. **54** 08LA01 (2015).
15) Y. Fujita, P. Walke, S. De Feyter, and H. Uji-i, Jpn. J. Appl. Phys. **55**, 08NA02 (2016).
16) K. Itaya and E. Tomita, Surface Science **201**, L507 (1988).
17) K. Gentz and K. Wandelt, Chimia (Aarau) **66**, 44 (2012).
18) S. Yoshimoto and K. Itaya, Annu. Rev. Anal. Chem. **6**, 213 (2013).
19) T. Takami, e-J. Surf. Sci. Nanotech. **12**, 157 (2014).
20) S. Taniguchi, Japan Patent 18561 (1978).
21) T. Suzuki and K. Ogawa, Japan Patent 246400 (1989).
22) L. Libioulle, Y.Houbion, and J.-M. Gilles, Rev. Sci. Instrum. **66**, 97 (1995).
23) I. H. Musselman and P. E. Russell, J. Vac. Sci. Technol. **A8**, 3558 (1990).
24) A. J. Nam, A. Teren, T. A. Lusby, and A. J. Melmed, J. Vac. Sci. Technol. **B13**, 1556 (1995).
25) A. Czerepak, Ph.D. Thesis, Physics Department, University of Notre Dame (2011); available from http://physics.nd.edu/assets/118523/.
26) M. Zhang and X. W. Lian, Materials **9** (2016) 233.
27) C.M.Vitus, H. S. Isaacs, V. Schroeder, "*A study of the electrochemical behavior in tungsten and caustic solutions and platinum/iridium in chloride solutions, informal report*", BNL-61136, p.19 (1994) [DOI:10.2172/10109621, Available online at www.osti.gov/scitech/ servlets/ purl/10109621/].
28) L. Libioulle, Y. Houbion, and J. –M. Gilles, Rev. Sci. Instrum., **66**, 97 (1995).
29) M. Kupper, Bachelor Thesis, Graz University of Technology, Graz (2012).
30) A. H. Sørensen, U. Hvid, M. W. Mortensen, and K. A. Mørch, Rev. Sci. Instrum., **70**, 3059 (1999).